Journal of Molecular Structure 1114 (2016) 84–94

Contents lists available at ScienceDirect

Journal of Molecular Structure

journal homepage: http://www.elsevier.com/locate/molstruc

# Design, synthesis, α-glucosidase inhibitory activity, molecular docking and QSAR studies of benzimidazole derivatives

Leila Dinparast [a, b], Hassan Valizadeh [b, *], Mir Babak Bahadori [c], Somaieh Soltani [d], Behvar Asghari [e], Mohammad-Reza Rashidi [a]

[a] Pharmacy Faculty, Tabriz University of Medical Sciences, Tabriz, Iran
[b] Organic Chemistry and Phytochemistry Research Laboratory, Faculty of Sciences, Azarbaijan Shahid Madani University, Tabriz, Iran
[c] Research Center for Pharmaceutical Nanotechnology, Tabriz University of Medical Sciences, Tabriz, Iran
[d] Drug Applied Research Center and Pharmacy Faculty, Tabriz University of Medical Sciences, Tabriz, Iran
[e] Department of Plant Production and Breeding Engineering, Faculty of Engineering and Technology, Imam Khomeini International University, Qazvin, Iran

ARTICLE INFO

*Article history:*
Received 8 November 2015
Received in revised form
28 January 2016
Accepted 2 February 2016
Available online xxx

*Keywords:*
Benzimidazole
Green synthesis
Spectroscopic data
α-Glucosidase
Molecular docking
QSAR

ABSTRACT

In this study the green, one-pot, solvent-free and selective synthesis of benzimidazole derivatives is reported. The reactions were catalyzed by ZnO/MgO containing ZnO nanoparticles as a highly effective, non-toxic and environmentally friendly catalyst. The structure of synthesized benzimidazoles was characterized using spectroscopic technics (FT-IR, $^{1}$HNMR, $^{13}$CNMR). Synthesized compounds were evaluated for their α-glucosidase inhibitory potential. Compounds **3c**, **3e**, **3l** and **4n** were potent inhibitors with $IC_{50}$ values ranging from 60.7 to 168.4 μM. *In silico* studies were performed to explore the binding modes and interactions between enzyme and synthesized benzimidazoles. Developed linear QSAR model based on density and molecular weight could predict bioactivity of newly synthesized compounds well. Molecular docking studies revealed the availability of some hydrophobic interactions. In addition, the bioactivity of most potent compounds had good correlation with estimated free energy of binding ($\Delta G_{binding}$) which was calculated according to docked best conformations.



## 1. Introduction

Benzimidazole and its derivatives are important *N*-Containing heterocyclic compounds in organic chemistry. They exhibit pharmaceutical and biological activities such as antiulcer [1], antihypertensive [2], antifungal [3–5], anticancer [6], anthelmintic [7], antibacterial [8], cytotoxic and antitumor [9], DNA binding [10], enzyme inhibition [11,12] and HIV-1-induced cytopathic inhibitor [13]. In addition, these compounds have been used as organic ligands [14,15], functional materials [16,17], dyes [16], chemosensing [18], fluorescence reagents [19], and in corrosion science [10,20,21]. Therefore, the synthesis of these heterocycles has always been of great interest to organic and medicinal chemists. Chemical structures of some important benzimidazoles with therapeutic applications are presented in Fig. 1.

Different synthesis strategies have been reported for the synthesis of benzimidazoles using $ZrCl_4$ [22], CuCl [23], $H_2O_2$/HCl [24], hypervalent iodine as oxidant [25], oxalic acid [26], *p*-toluenesulphonic acid [27], $SOCl_2/SiO_2$ [28], L-Praline [29], Sulphamic acid [30], and Zeolite [31]. However, many of these reported methods suffer from some drawbacks such as drastic reaction conditions, long reaction time, poor yield, formation of mixture of products, use of toxic, homogeneous and expensive catalysts and hazardous organic solvents. Recently, metal oxides have attracted considerable attention of synthetic chemists and have been used as heterogeneous catalysts in different organic reactions [32,33]. These compounds are non-toxic and stable in various reaction conditions [34,35]. Nanometal oxides have higher catalytic activity than their bulk counterparts due to high surface area to volume ratio [36]. Metal oxides surfaces show both Lewis acid/Lewis base properties and they are very good absorbents of various organic compounds. ZnO/MgO containing ZnO nanoparticles is non-toxic, environmentally friendly, easily available and inexpensive solid catalysts which has been widely used as an efficient heterogeneous catalyst in organic reactions in ionic liquid [37,38]. It is generally not corrosive and do

* Corresponding author. Kilometer 35, Tabriz/Azarshahr Road, P.O.Box: 53714-161, Tabriz, Iran.
*E-mail address:* h-valizadeh@azaruniv.edu (H. Valizadeh).

http://dx.doi.org/10.1016/j.molstruc.2016.02.005
0022-2860/

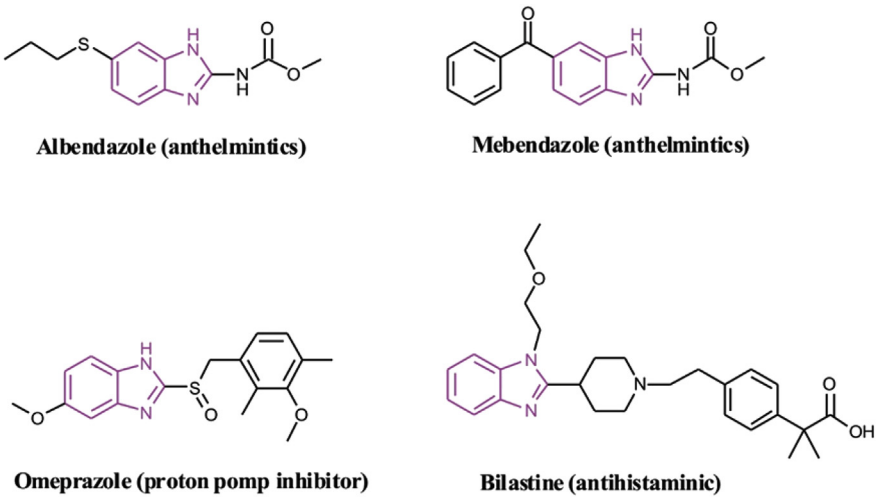


**Fig. 1.** Structures of some pharmacologically important benzimidazoles.

not produce problematic side products.

Ionic liquids are being classified as green solvents because of their unique physicochemical properties [39]. We reported the synthesis of 4*H*-pyrans and coumarins using ZnO/MgO containing ZnO nanoparticles (nano-ZnO/MgO) as an effective heterogeneous base catalyst in [bmim]$BF_4$ [40].

Diabetes Mellitus (DM), as a metabolic disease is a growing health problem. Currently, 250 million people are living with diabetes in the world and this number is predict to be more than 366 million by 2030, based on the WHO reports [41]. As a result of diabetes, high concentration of the glucose in the blood (hyperglycemia) damages many of the body's organs, especially the nerves and blood vessel [42]. α-Glucosidase hydrolyzes terminal non-reducing 1–4 linked α-glucose residues to release a single α-glucose molecule [43]. Acarbose is the first member of α-glucosidase inhibitors which currently approved for the treatment of type 2 diabetes. The control of the glucose levels in the blood by inhibition of carbohydrate-hydrolyzing enzymes, such as α-glucosidase is one of the therapeutic approaches for the treatment of diabetic patients [41,44,45]. In addition, α-glucosidase inhibitors are known to have antiviral, anticancer, anti-HIV and antitumor activities [46–48]. Therefore, design and the synthesis of organic compounds with the α-glucosidase inhibitory activity is an important area of medicinal chemistry.

Literature review showed that there are just three studies on α-glucosidase inhibitory activity of benzimidazole derivatives. Very recently, Asghari et al. reported the synthesis of new benzimidazole and pyrimidine derivatives as α-glucosidase inhibitors [49]. Menteşe et al. reported the synthesis of benzimidazole derivatives containing triazole, thiadiazole, oxadiazole, and morpholine rings which show the α-glucosidase inhibitory activity [50]. Also, Ashok et al. reported the synthesis, α-glucosidase inhibitory activity and cytotoxicity of benzimidazole derivatives [51].

In continuation of our interest in developing environmentally friendly and green chemistry [52–54], herein we report selective, one-pot and solvent-free synthesis of benzimidazole derivatives in high to excellent yields (Scheme 1). Synthesized derivatives were tested for *in vitro* α-glucosidase inhibitory activity. Afterward, *in silico* molecular docking studies were performed to further investigate the interactions and binding energies between the ligands and macromolecule. QSAR models were developed to investigate the relationship between the observed bioactivity and the structural and physicochemical properties of synthesized benzimidazoles.

## 2. Results and discussion

### 2.1. Chemistry

As a model reaction, 4-nitrobenzaldehyde and *o*-phenylenediamine were reacted in variety of reaction conditions (Table 1). In a first attempt, 4-nitrobenzaldehyde (1 mmol) and *o*-phenylenediamine (1 mmol) were added to [bmim]Cl at 40 °C and stirred for 120 min. Work-up of the reaction mixture afforded the products **3a** and **4a** in 35 and 20% yields, respectively (Table 1, entry 1). Study of the procedure at higher temperatures showed that just the reaction times decrease under these conditions (Table 1, entries 2, 3). The present condensation reaction needs a catalyst with dual acid/base characteristics. The Lewis base for *o*-phenylenediamine activation and the Lewis acid for benzaldehyde activation. Accordingly, catalytic activity of nano-ZnO/MgO was investigated in this reaction and it was found that the reaction was complete in a shorter time, with significantly higher yields (Table 1, entry 4). In addition, the ratio of **3a**/**4a** was increased in the presence of nano-ZnO/MgO and selectivity in the products of the reaction was observed. Nano-ZnO/MgO was prepared according to the literature [55]. The SEM image of nano-ZnO/MgO was shown in Fig. 2. Selectivity in products was increased in higher temperatures (Table 1, entry 5). Using of other ionic liquids such as [bmim]Br, [bmim]$BF_4$ and [bmim]$PF_6$ has no significant effect in the yield of the products, but reaction time in [bmim]Cl was shorter than other ionic liquids (Table 1, entries 8–10). Performing of the reaction in the absence of any solvent or ionic liquid and also in other conventional organic solvents such as toluene, dichloromethane and acetonitrile did not give corresponding products after long reaction time (Table 1, entries 11–14). As a consequence, [bmim]Cl was found to be the best solvent. The model reaction was optimized by using various combinations of nano-ZnO/MgO, ionic liquid and the reactants at different temperatures. It was found that the best yield of the product and good selectivity were obtained using 1/1 molar ratios of 4-nitrobenzaldehyde and *o*-phenylenediamine in the presence of nano-ZnO/MgO (15 mol %) at 60 °C (Table 1, entry 7).

Under these optimized reaction conditions, the reaction of several benzaldehyde derivatives with *o*-phenylenediamine derivatives was also examined. The corresponding benzimidazoles were obtained and isolated in good yields (Table 2). A slight increase in yield can be seen in benzaldehyde derivatives with

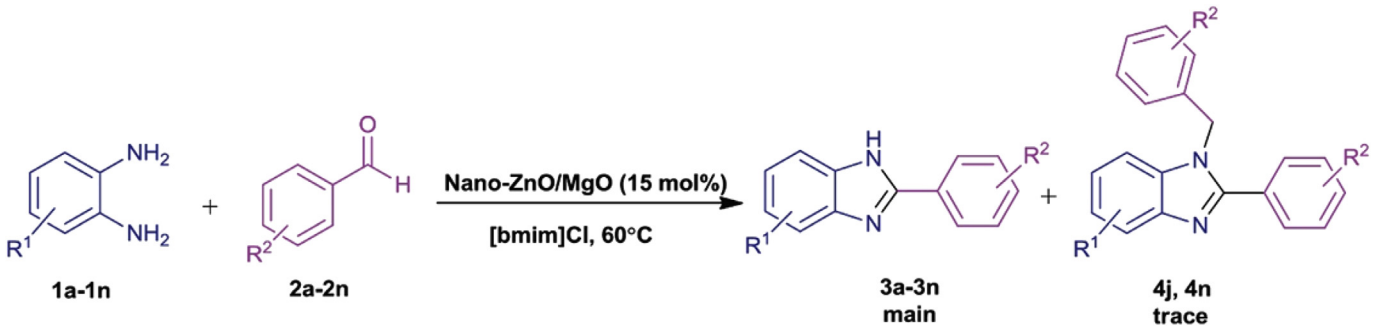


**Scheme 1.** Selective synthesis of benzimidazole derivatives in the presence of nano-ZnO/MgO in [bmim]Cl.

**Table 1**
Reaction of 4-nitrobenzaldehyde (1 mmol) with *o*-phenylenediamine (1 mmol) in the different reaction conditions.

| Entry | Solvent | Temperature (°C) | Catalyst (mol %) | Time (min) | Yield[a] (%) **3a** | Yield[a] (%) **4a** |
|---|---|---|---|---|---|---|
| 1 | [bmim]Cl | 40 | – | 120 | 35 | 20 |
| 2 | [bmim]Cl | 50 | – | 100 | 40 | 25 |
| 3 | [bmim]Cl | 60 | – | 60 | 45 | 30 |
| 4 | [bmim]Cl | 50 | Nano-ZnO/MgO (25) | 30 | 80 | 5 |
| 5 | [bmim]Cl | 60 | Nano-ZnO/MgO (25) | 15 | 87 | – |
| 6 | [bmim]Cl | 70 | Nano-ZnO/MgO (25) | 15 | 87 | – |
| 7 | [bmim]Cl | 60 | Nano-ZnO/MgO (15) | 15 | 87 | – |
| 8 | [bmim]$BF_4$ | 60 | Nano-ZnO/MgO (15) | 25 | 78 | – |
| 9 | [bmim]$PF_6$ | 60 | Nano-ZnO/MgO (15) | 25 | 70 | 5 |
| 10 | [bmim]Br | 60 | Nano-ZnO/MgO (15) | 25 | 75 | 5 |
| 11 | Toluene | 60 | Nano-ZnO/MgO (15) | 120 | 15 | 10 |
| 12 | $CH_2Cl_2$ | 60 | Nano-ZnO/MgO (15) | 120 | – | – |
| 13 | $CH_3CN$ | 60 | Nano-ZnO/MgO (15) | 120 | 20 | 15 |
| 14 | – | 60 | Nano-ZnO/MgO (15) | 120 | – | – |

[a] Isolated yields.

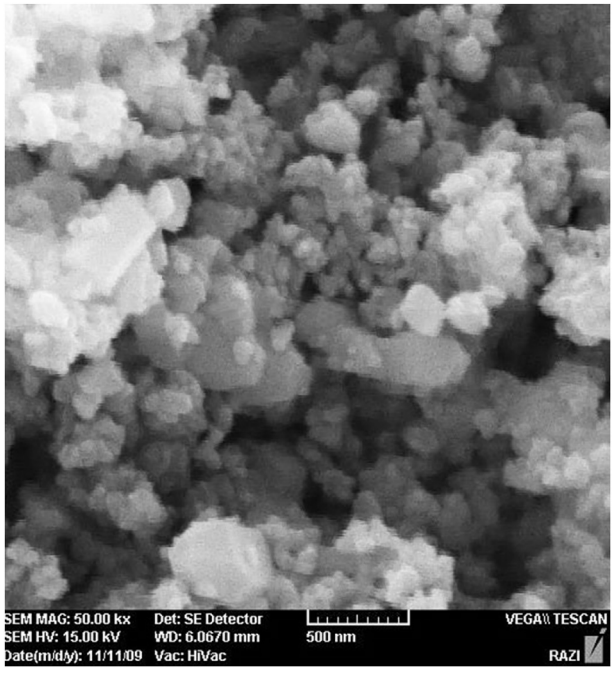


**Fig. 2.** The SEM image of nano-ZnO/MgO.

electron-withdrawing substituents such as nitro and chloro groups and *o*-phenylenediamines containing electron donating groups such as methyl (Table 2). The efficiency of catalyst in this condensation reaction supported by dual Lewis acid and Lewis base characteristics of ZnO/MgO containing ZnO nanoparticles. Nano-ZnO/MgO has both Lewis base and Lewis acid moieties. The Lewis base site of catalyst ($O^{2-}/O^{2-}$) activates *o*-phenylenediamine and the Lewis acid ($Mg^{+2}/Zn^{2+}$) site activates benzaldehyde.

To the best of our knowledge, this is the first report for the selective synthesis of benzimidazole derivatives in the presence of nano-ZnO/MgO. Moreover, based on the literature survey, molecular docking and QSAR studies of benzimidazole derivatives with the α-glucosidase inhibitory activity are reported here for the first time.

A possible mechanism for the formation of product **3** in ionic liquid in the presence of nano-ZnO/MgO catalyst is shown in Scheme 2. The reaction proceeds via dual activation of substrates by nanometal oxide catalyst. At first, benzaldehyde and *o*-phenylenediamine are activated by nano-ZnO/MgO. Intermediate **I** is resulted by nucleophilic attack of *o*-phenylenediamine **1** to benzaldehyde **2**. Subsequently, coordination of nitrogen to nano-ZnO/MgO facilitates intramolecular cyclization of intermediate **I** and the formation of intermediate **II**. Deprotonation of intermediate **II** results the product **3**.

### 2.2. α-Glucosidase inhibitory activity

α-Glucosidase inhibitors are used for the treatment of metabolic disorders like diabetes. Such compounds decrease the level of glucose in the blood. In the present study, the synthesized benzimidazole derivatives were screened for their *in vitro* α-glucosidase inhibitory potential (except **3j** and **4j**) as shown in Fig. 3. Compounds with inhibition more than 50% at concentration of 50 μg/mL were further evaluated for determining of their $IC_{50}$ values. Our findings revealed that compounds **3c**, **3e**, **3l** and **4n** have moderate to high α-glucosidase inhibitory activity with $IC_{50}$ values ranged

**Table 2**
The synthesized derivatives of benzimidazole in the presence of nano-ZnO/MgO as an efficient catalyst.

| Entry | $R^1$ | $R^2$ | Products | Prod. no. | Time (min) | Yield[a] % |
|---|---|---|---|---|---|---|
| 1 | H | 4-$NO_2$ | 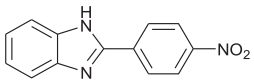 | **3a** | 15 | 87 |
| 2 | H | 3-$NO_2$ | 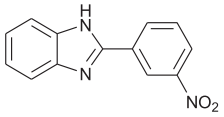 | **3b** | 15 | 80 |
| 3 | H | 4-$OCH_3$ | 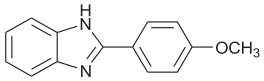 | **3c** | 20 | 79 |
| 4 | 4-Me | 4-$NO_2$ | 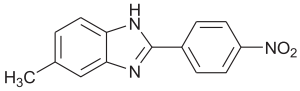 | **3d** | 15 | 90 |
| 5 | 4-$CH_3$ | 4-$OCH_3$ | 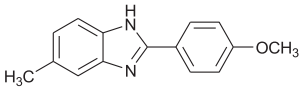 | **3e** | 17 | 80 |
| 6 | 4-$CH_3$ | 4-Cl | 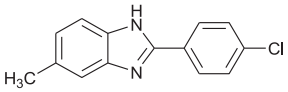 | **3f** | 15 | 83 |
| 7 | 4-Br | 4-$NO_2$ | 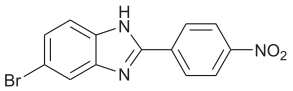 | **3g** | 15 | 88 |
| 8 | 4-Br | 4-$OCH_3$ | 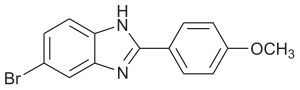 | **3h** | 20 | 75 |
| 9 | 4-Br | 4-Cl | 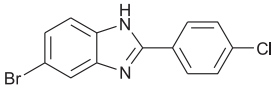 | **3i** | 17 | 78 |
| 10 | 4-Cl | 4-$NO_2$ | 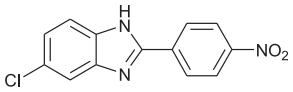 | **3j** | 15 | 88 |
| 11 | 4-Cl | 3-$NO_2$ | 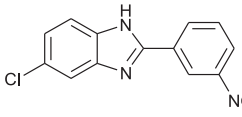 | **3k** | 15 | 78 |
| 12 | 4-Cl | 4-$OCH_3$ | 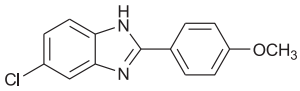 | **3l** | 20 | 77 |
| 13 | 4-Cl | 4-Cl | 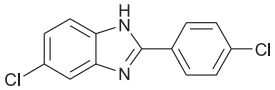 | **3m** | 15 | 80 |
| 14 | 4-Cl | 4-CN | 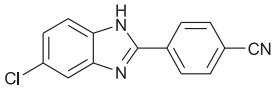 | **3n** | 15 | 88 |

[a] Isolated yields.

from 60.7 to 168.4 μM (Table 3). All of these potent compounds exhibited their activity in a concentration dependent manner (Fig. 4). Acarbose ($IC_{50}$ = 47.7 μM) was used as the standard drug. A wide range of natural or synthetic compounds like flavonoids, carbohydrates, steroids, coumarins, etc., have demonstrated to be α-glucosidase inhibitor. Literature review showed that there is very limited information on α-glucosidase inhibitory potential of benzimidazole derivatives. Our findings confirmed the efficacy of this class of compounds for future drug discovery investigations.

### 2.3. Molecular docking studies

The results of molecular docking of benzimidazole derivatives are given in Table 4. According to the experimental data, the most

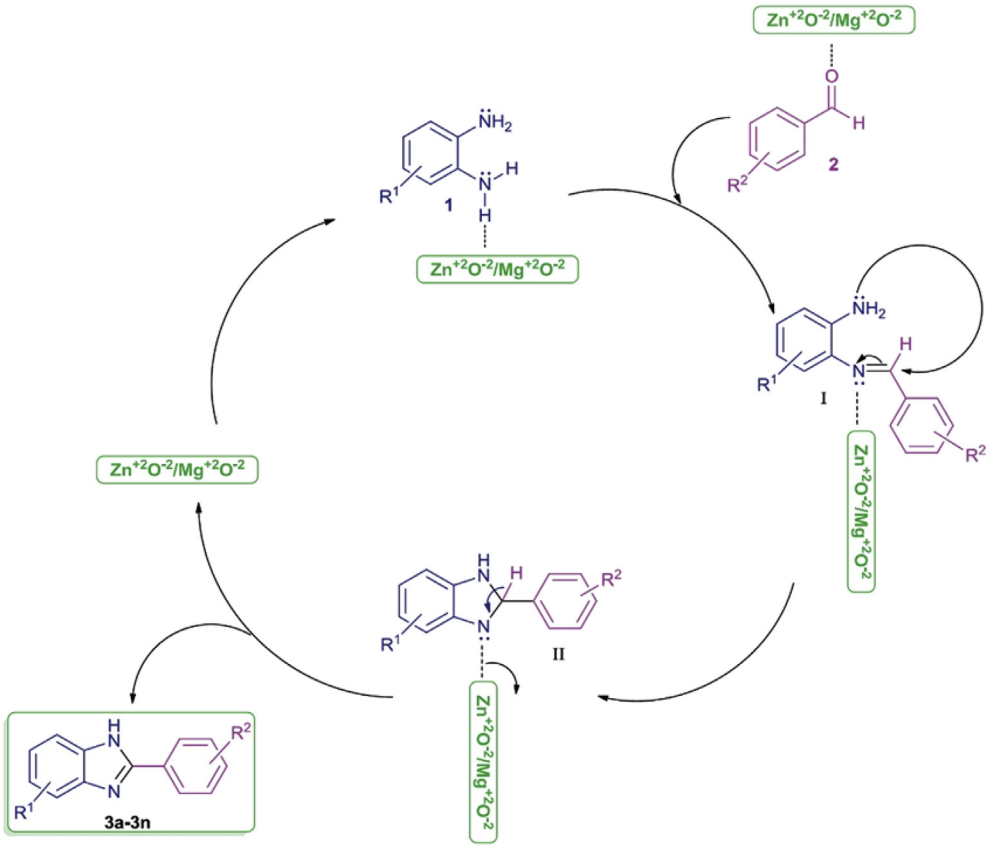


**Scheme 2.** The plausible mechanism of the reaction.

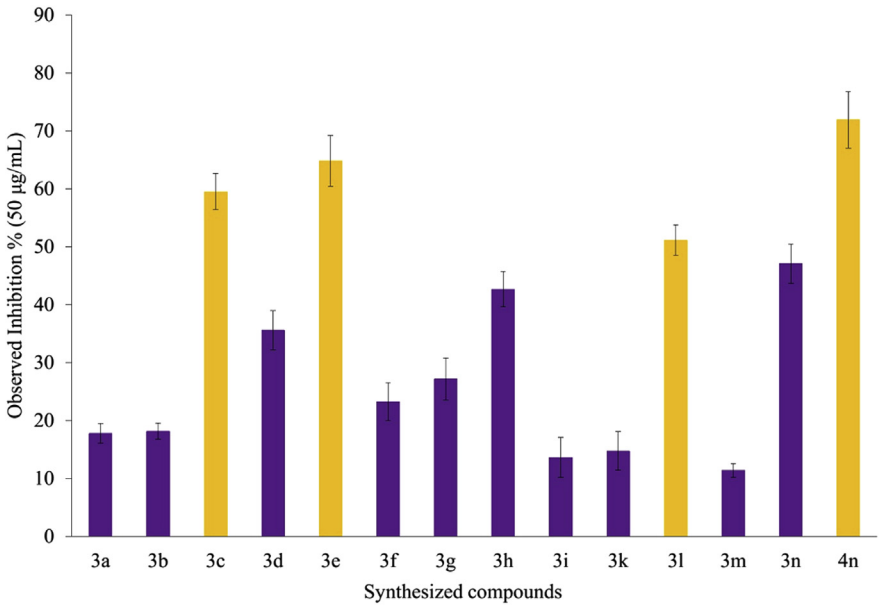


**Fig. 3.** α-Glucosidase inhibitory activity of synthesized compounds.

active derivative (**4n**) has similar inhibitory activity to the reference inhibitor (acarbose). The results of docking analysis showed that binding affinity of acarbose ($\Delta G_{binding} = -8.5$ kcal/mol and four hydrogen bonds with HIS1584, ASP1526 and ASP1157) is higher than all tested compounds. This result is in agreement with *in vitro* observations. The observed $IC_{50}$ values of tested compounds revealed that the order of bioactivity is **4n** > **3e** > **3c** > **3l**. The same trend was obtained from docking studies. Fig. 5 shows superposition of docked compounds (**3c**, **3e**, **3l** and **4n**) in the active site of α-glucosidase. The important binding site amino acid residues

**Table 3**
α-Glucosidase inhibitory activity of synthesized compounds.[a]

| Compound | $IC_{50}$ (μg/mL) | $IC_{50}$ (μM) |
|---|---|---|
| 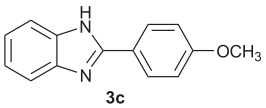 **3c** | 38.2 ± 2.1 | 165.9 ± 13.1 |
| 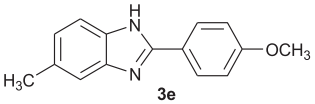 **3e** | 28.5 ± 0.4 | 119.7 ± 1.6 |
| 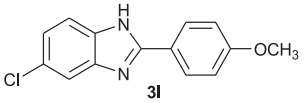 **3l** | 43.5 ± 0.9 | 168.4 ± 3.6 |
| 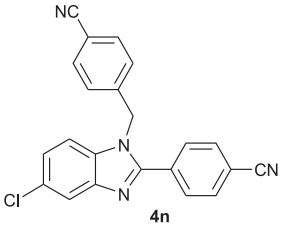 **4n** | 22.4 ± 0.6 | 60.7 ± 1.7 |
| Acarbose [b] | 30.8 ± 1.1 | 47.7 ± 1.7 |

[a] Values are mean ± SEM of three independent experiments.
[b] Standard drug.

which are involved in H-bond interactions with the potent compounds are ASP1526 and LYS1460. Top ranked conformation of **4n** created two hydrogen bond between nitrogen atom of compound and carboxylic and amine groups of ASP1526. Furthermore, several hydrophobic interactions were observed (Fig. 6) which stabilize the binding of compound **4n**. The estimated free energy of these interactions is −7.35 kcal/mol. Docking analysis of compound **3e** showed that oxygen atom of methoxy group on the benzene ring was involved in hydrogen bond with amine group of LYS1460. Also, there is another hydrogen bond between the −NH fragment of compound **3e** and carboxylic group of LYS1460 (Fig. 6). The results of *in silico* studies about **3c** and **3l** clarified that hydrogen bond was formed between the −NH fragments of the compounds and carboxylic group of ASP1526 (Fig. 6). In addition, in the case of **3l** the benzene ring was involved in a π-cation interaction with LYS1460. Comparing the estimated free energy of binding of benzimidazole derivatives with acarbose showed that compounds **3c**, **3e, 3l** and **4n** could be moderate to strong inhibitors.

Molecular weight, log *P* and molar refractivity were calculated (supplementary material, Table S1). Log *P*, molecular weight, H-donor and H-acceptor atoms of all compounds are within the Lipinski's rule of five. Moreover, molar refractivity of these compounds is in the standard range of the Lipinski's rule of five. These properties along with docking studies results suggested the suitability of potent derivatives (i.e. **3c**, **3e**, **3l** and **4n**) as oral drug candidates.

### 2.4. QSAR results

The best developed MLR model (Eq. (1)) showed that α-glucosidase inhibitory activity of synthesized benzimidazole compounds is affected by two molecular descriptors; i.e. molecular weight and density.

$$Inhibition\% = 0.267Mw - 117.99\,density + 128.1 \quad (1)$$

(N = 14, S. E. = 14.15, F = 0.83, *P*-value = 0.0075)

Inhibition percent of these compounds is positively correlated with the molecular weight whereas negatively correlated with density of the molecules. Based on the beta coefficients, density of compounds is more important parameter than the molecular weight. The parameters of developed QSAR model, experimental and predicted inhibition presents of benzimidazoles are given in Table 5. Fig. 7A shows the scatter plot of observed versus predicted inhibition percent. Regression coefficient and $Q^2$ of leave one out cross validation were 0.60 and 0.69, respectively which was acceptable according to Roy and Roy [56] rules for QSAR model validation in which they noted that the difference between $R^2$ and $Q^2$ values should be less than 0.3.

The correlation between the observed and predicted activities for potent compounds (inhibition % >45) shows that the developed model could predict bioactivity of the potent compounds significantly better than the weak compounds (Fig. 7B). Fig. 6C represents the correlation between the predicted inhibition percent and the experimental $IC_{50}$ values. According to the resulted correlation coefficient, the QSAR model could predict $IC_{50}$ values well.

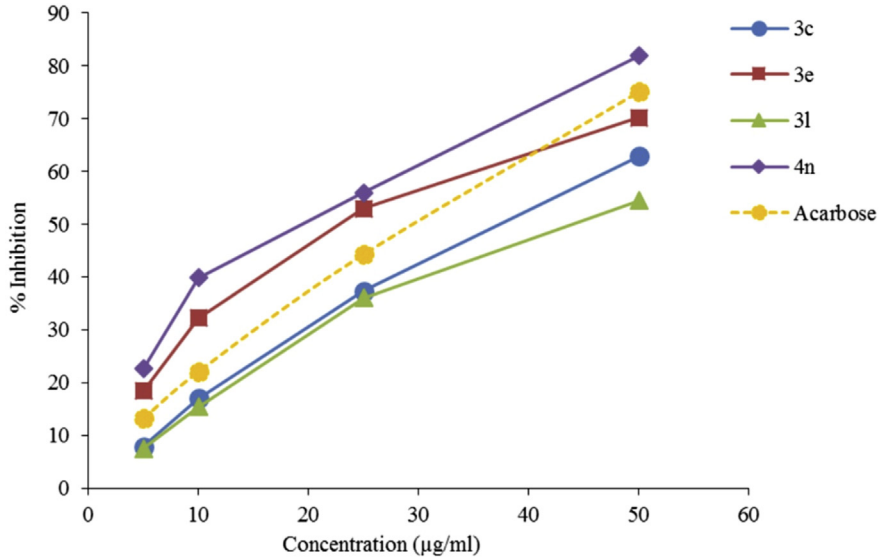


**Fig. 4.** α-Glucosidase activity of potent compounds (**3c**, **3e**, **3l** and **4n**) and acarbose. Values are mean of triplicates.

**Table 4**
The results of docking analysis.

| Products | Intermolecular energy (kcal/mol) | Estimated $\Delta G_{Binding}$ (kcal/mol) | $E_2$[a] (kcal/mol) | Electrostatic energy (kcal/mol) | Ligand efficiency (kcal/mol) | Torsional energy (kcal/mol) | Unbound energy (kcal/mol) | Active site residues | H-bonded residues and π-cation interactions |
|---|---|---|---|---|---|---|---|---|---|
| **3a** | −6.88 | −6.28 | −6.44 | −0.43 | −0.42 | 0.3 | −0.25 | TRP1355, MET1421, ARG1510, ASP1526, ASP1157, LYS1460 | – |
| **3b** | −6.34 | −5.74 | −6.01 | −0.33 | −0.43 | 0.3 | −0.25 | MET1421, ARG1510, PHE1427, ASP1157, LYS1460, PRO1159, ASP1526, PHE1559 | ARG1157 |
| **3c** | −7.30 | −6.70 | −7.08 | −0.22 | −0.31 | 0.6 | −0.29 | TRP1418, TRP1523, ARG1510, TRP1355, MET1421, ASP1157, PHE1427, ASP1526 | ASP1526 |
| **3d** | −6.83 | −6.23 | −6.45 | −0.37 | −0.35 | 0.6 | −0.32 | PHE1559, ASP1526, TRP11418, ARG1510, MET1421, ASP1157, LYS1460 | – |
| **3e** | −7.34 | −6.74 | −7.06 | −0.28 | −0.32 | 0.6 | −0.029 | TRP1418, TRP1355, ARG1510, PHE1427, ASP1157, LYS1460, TRP1369, ASP1526 | LYS1460 |
| **3f** | −7.26 | −6.96 | −7.14 | −0.13 | −0.41 | 0.3 | −0.25 | HIS1584, PHE1559, ASP1526, ARG1510, TRP1355, PHE1427, TRP1369, ASP1157 | ASP1526 |
| **3g** | −7.18 | −6.59 | −7.00 | −0.18 | −0.38 | 0.6 | −0.28 | PHE1559, TRP1418, TRP1523, TRP1355, ARG1510, MET1421, ASP,1157, PHE1427, LYS1460, TRP1369 | – |
| **3h** | −7.45 | −6.85 | −7.28 | −0.17 | −0.35 | 0.6 | −0.31 | TRP1418, PHE1559, ASP1526, ARG110, TRP1355, MET1421, PRO1159, TRP1369, ASP1157, PHE1427, LYS1450 | ASP1126 π-cation interaction (LYS1460) |
| **3i** | −7.53 | −7.23 | −7.36 | −0.17 | −0.33 | 0.6 | −0.31 | HIS1584, PHE1559, ASP1526, ARG1510, TRP1355, ASP1157, PHE1427, LYS1460, TRP1369 | ASP1526 |
| **3k** | −6.49 | −5.89 | −6.75 | +0.26 | −0.38 | 0.3 | −0.25 | PHE 1559, TRP1418, TRP1355, ARG1510, PHE1427, ASP1157, LYS1460, PRO1159, ASP1526 | LYS1460 |
| **3l** | −7.33 | −6.73 | −7.14 | −0.19 | −0.37 | 0.6 | −0.28 | TRP1418, PHE1559, ASP1526, PRO1159, ARG1510, TRP1355, MET1421, ASP1157, PHE1427, LYS1460, TRP1369 | ASP1526 π-cation interaction (LYS1460) |
| **3m** | −7.44 | −7.14 | −7.24 | −0.19 | −0.39 | 0.6 | −0.29 | HIS1584, PHE1559, ASP1526, ARG1510, TRP1355, PHE1427, ASP1157, TRP1369 | ASP1526 |
| **3n** | −6.98 | −7.07 | −6.77 | −0.09 | −0.37 | 0.6 | −0.28 | TRP1418, PHE1559, MET1421, TRP1355, PHE1427, LYS1460, TRP1369, ASP1157, ARG1510 | – |
| **4n** | −8.24 | −7.35 | −8.24 | −0.01 | −0.29 | 0.89 | −1.32 | TRP1418, ASP1420, TRP1355, MET1421, ARG1510,PHE1559, ASP1526, PHE1560, PRO1159, ASP1157, TRP1369, LYS1460 | ASP1526 |
| **Acarbose** | −15.06 | −8.50 | −11.68 | −3.38 | −0.19 | 6.56 | −0.9 | HIS1584, ASP1279, ILE1280, PHE1559, ARG1510, TRP1355, MET1421, ASP1157, ASP1526, ARG1510, LYS1460, PRO1159, TRP1369 | HIS1584, ASP1526, ASP1157 (2) |

[a] $E_2$ = vdW + Hbond + desolv Energy.

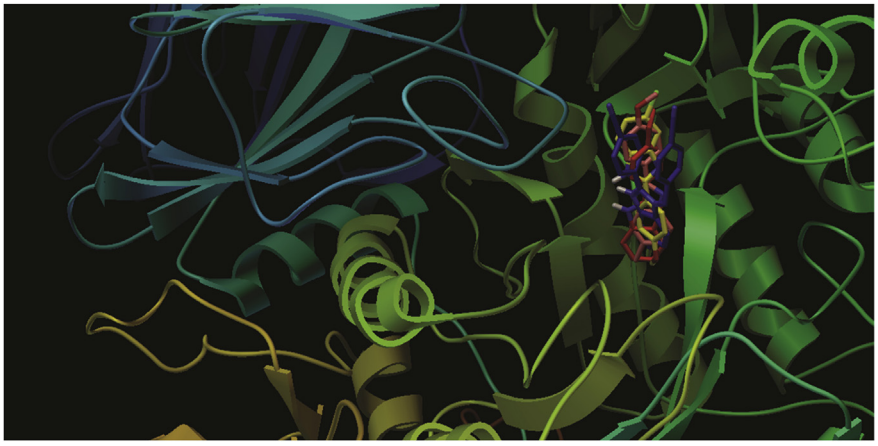

**Fig. 5.** Superposition of docked compounds (**3c**, **3e**, **3l** and **4n**) in the active site of α-glucosidase.

## 3. Experimental

### 3.1. General experimental procedures

Infrared spectra were recorded on a Perkin Elmer FT-IR spectrometer using KBr pellets. $^1$HNMR and $^{13}$CNMR spectra were recorded on a Bruker Avance AC- 300 MHz Spectrometer. All melting points were measured in open glass capillaries using a Stuart melting point apparatus. All reagents for synthesis were purchased from Merck and used without further purification. $CDCl_3$ and MeOD-$d_4$ were used as the deuterated solvents and TMS as an internal standard. α-Glucosidase type I from Baker Yeast (EC 3.2.1.20) and 4-nitrophenyl-α-D-glucopyranoside (*p*NPG) were obtained from Sigma–Aldrich. Scanning electron microscopy

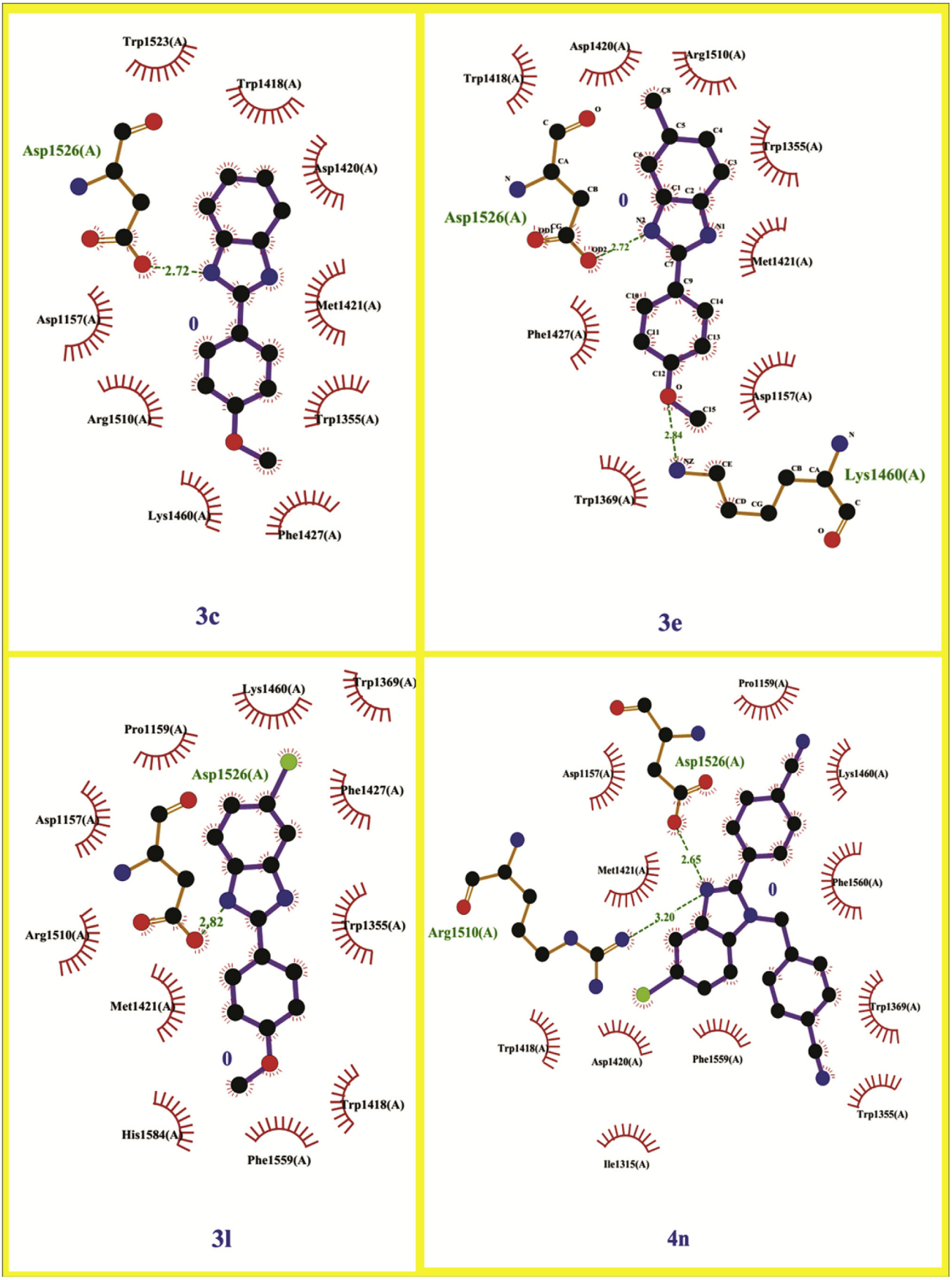


**Fig. 6.** Predicted binding mode and interactions of compounds **3c**, **3e**, **3l** and **4n** in the active site of α-glucosidase.

**Table 5**
The parameters of developed QSAR model and the experimental and predicted bioactivity of the synthesized benzimidazoles according to Eq. (1).

| Compound | Exp. Inhibition % | Pred. Inhibition % | Molecular weight | Density ($gcm^{-3}$) |
|---|---|---|---|---|
| **3m** | 11.37 | 30.06 | 263.12 | 1.427 |
| **3i** | 13.63 | 17.88 | 307.57 | 1.631 |
| **3k** | 14.70 | 26.04 | 273.67 | 1.485 |
| **3a** | 17.77 | 28.16 | 239.23 | 1.389 |
| **3b** | 18.13 | 28.16 | 239.23 | 1.389 |
| **3f** | 23.27 | 41.24 | 242.7 | 1.286 |
| **3g** | 27.17 | 13.97 | 318.13 | 1.688 |
| **3d** | 35.57 | 37.34 | 253.26 | 1.343 |
| **3h** | 42.63 | 30.85 | 303.15 | 1.511 |
| **3n** | 47.07 | 28.37 | 253.69 | 1.42 |
| **3l** | 51.10 | 41.86 | 258.7 | 1.317 |
| **3c** | 59.50 | 44.57 | 224.26 | 1.216 |
| **3e** | 64.83 | 52.09 | 238.28 | 1.184 |
| **4n** | 71.90 | 78.03 | 368.82 | 1.26 |

(SEM) (VEGA/TESCAN) was used for morphology study of ZnO/MgO nanoparticles. Mass spectra, using electron ionization (EI)-mass spectrometry (MS), were recorded on a Shimadzu GCMS-QP-2000A mass spectrometer. Elemental analyses were conducted using the Perkin–Elmer 240C elemental analyzer, their results were found to be in good agreement with the calculated values. The ultraviolet visible spectra of synthesized benzimidazoles were recorded in acetonitrile as the solvent using Shimadzu 2550 UV/Vis spectrophotometer in the range of 200–700 nm at room temperature in quarts cell 1 cm.

### 3.2. Methods

#### 3.2.1. General procedure for selective synthesis of benzimidazole derivatives

Benzaldehyde derivatives (1 mmol), *o*-phenylenediamine (1 mmol), [bmim]Cl (2 g) and ZnO/MgO nanoparticles were mixed thoroughly. The reaction mixture was stirred at 70 °C for the time as shown in Table 2. The progress of the reaction was monitored by TLC (using ethyl acetate: *n*-hexane 1:3 as eluent). After the completion of the reaction, the mixture was extracted with ethyl acetate. Evaporation of the solvent using a rotary evaporator at 45 °C provided the crude product, which was further purified by column chromatography (ethyl acetate: *n*-hexane 1:3) to afford the final pure product.

### 3.3. α-Glucosidase inhibitory activity

α-Glucosidase inhibitory activity of the synthesized compounds was measured according to the previously published procedure [57] with some modifications. Briefly, 20 μL of 0.5 unit/mL α-glucosidase enzyme solution was mixed with 120 μL of 100 mM potassium phosphate buffer (pH = 6.9) and 10 μL of the compound

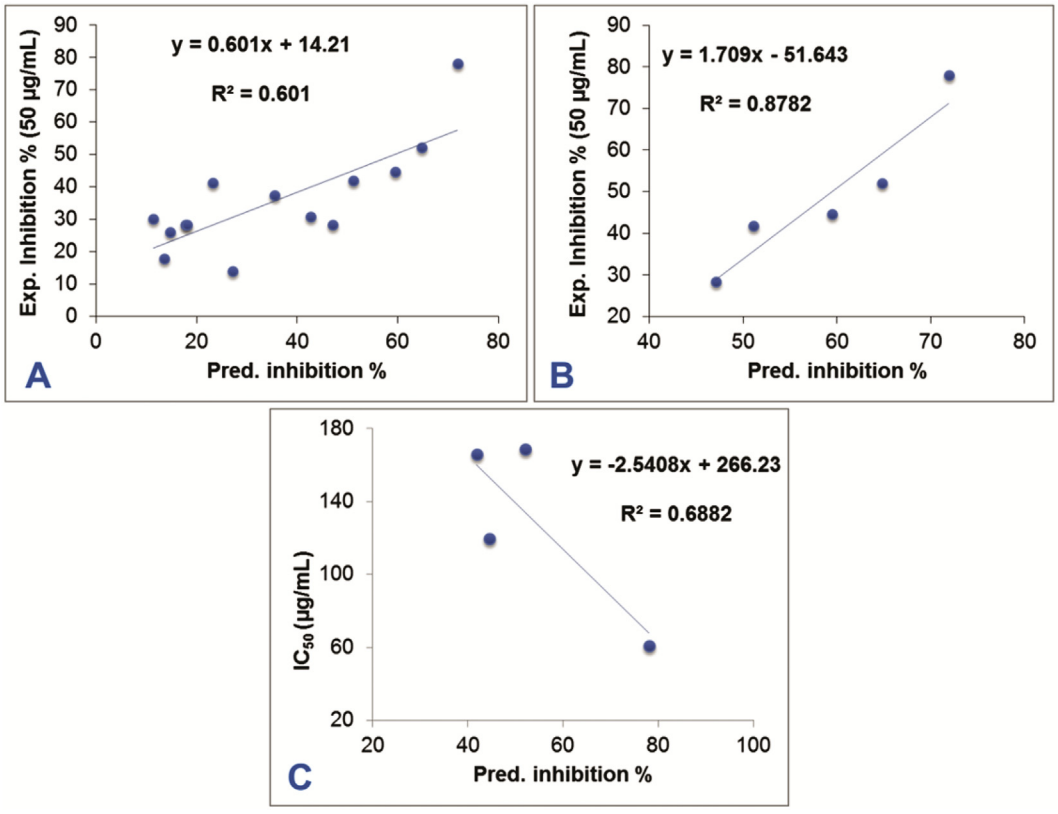


**Fig. 7.** . A) The experimental inhibition percent versus predicted data according to Eq. (1). B) The correlation graph between the experimental inhibition percent of potent compounds (>45%) (at 50 μg/mL) and predicted data. C) The correlation graph between the predicted inhibition percent and $IC_{50}$ values.

sample for final concentration of 50 μg/mL in the reaction mixture. Acarbose was used as standard positive control. The mixture was incubated at 37 °C for 15 min and then enzymatic reaction was initiated by adding 20 μL of 5 mM 4-nitrophenyl-α-D-glucopyranoside (*p*NPG) in buffer. The plates were incubated at 37 °C for another 15 min and the reaction was stopped by addition of 80 μL sodium carbonate solution (0.2 M). Finally, the absorbance of 4-nitrophenol released from *p*NPG was measured at 405 nm. The system without α-glucosidase was used as blank for correcting the background absorbance. The increasing of absorbance was compared with the control (buffer instead of sample solution) to calculate the inhibitory activity. The enzyme inhibition rate of the samples was calculated using the following formula:

$$\%\,Inhibition = [(Absorbance\ control - Absorbance\ sample)/Absorbance\ control] \times 100$$

Afterward, derivatives with inhibition percent more than 50 in above concentration were tested in lower concentrations (5, 10, 25 and 50 μg/mL) for calculation of $IC_{50}$ values. All of the experiments were carried out in triplicates. $IC_{50}$ values were calculated and expressed as mean ± SEM (Table 3).

### 3.4. Computational methods

#### 3.4.1. Software

The molecular geometry optimization of 3D structures of compounds was carried out at the Hartree–Fock (HF) level with 3-21G basis set using Gaussian 03 program package [58]. The molecular docking of synthesized benzimidazoles was performed using AutoDock 4.2 software [59]. MLR model was developed using the SPSS software. The dipole moment and stability energy of optimized molecules was calculated by Gaussian 03 program. Physicochemical properties i.e. log *P*, log *D*, molar refractivity, surface tension, density and polarizability were calculated by ACD/Labs program while the surface area was calculated using Hyper Chem 7 software.

#### 3.4.2. Molecular docking

The crystal structures of C-terminal domain of human intestinal α-glucosidase (PDB code:3TOP, complex with acarbose) was downloaded from Brookhaven protein database. Water molecules were removed from enzyme structure whereas, the polar hydrogen atoms, Kollman and Gasteiger charges were added to amino acid residues of protein structure using Autodock Tools (ADT, version 1.5.6) [60]. The required pdbqt format of receptor and ligands were obtained using the same software. Optimized structures of ligands with the minimized energy were subjected for molecular docking studies using Lamarckian genetic algorithm method (LGA) with 200 run for each docking. The population size and maximum number of evaluation (medium) were set at 150 and 2500000, respectively. The maximum number of generation was 27000. The grid box for the C-terminal α-glucosidase was place at the center of acarbose with x, y, and z coordinates of −28.191, 32.654 and 24.654 Å [61]. The number of points in x, y and z dimensions was 32 × 32 × 32 in C-terminal domain. The grid spacing was set in 0.375 Å.

#### 3.4.3. Quantitative structure activity relationship (QSAR)

*3.4.3.1. Data preparation.* Synthesized bezimidazole compounds (14 data point) with experimental enzyme inhibition percent was used as a data set in the present QSAR study. The observed bioactivity along with the calculated descriptors is given in the supplementary material, Table S1.

*3.4.3.2. Model development.* Best descriptors were selected using stepwise regression method and the selected descriptors were used to develop a linear model using multiple linear regression analysis [62–64]. Regression coefficient, standard error of estimate and F value along with the Leave one out cross-validation (LOOCV) method was used to check the prediction capability of the developed model.

## 4. Conclusions

A series of benzimidazole derivatives were synthesized selectively using ZnO/MgO containing ZnO nanoparticles. The use of non-toxic, recyclable and cheap catalyst and ionic liquid makes this synthesis method green and economical. Other advantages of this method were one-pot, solvent-free and mild reaction conditions and high yields of products. The structure of the synthesized compounds was investigated using spectroscopic data. Synthesized benzimidazoles were evaluated for their α-glucosidase inhibitory potential. Compounds **3c**, **3e**, **3l** and **4n** showed moderate to high activity. *In silico* studies were also performed to recognize the binding modes and molecular interactions of these compounds. Good accordance was found between the experimental data and docking results. A QSAR model was established to find the correlation between observed bioactivity and structural properties of synthesized derivatives. This model showed linear relationship between the experimental inhibition percent of compounds with molecular weight and density of the molecules. Our findings indicated that this class of compounds could be considered as potent α-glucosidase inhibitors. So, further studies on more derivatives and pharmacological evaluations are warranted.

## Disclosure of interest

The authors declare no conflicts of interest concerning this article.

## Acknowledgment

The partial financial assistance from the Research Vice Chancellor of Azarbaijan Shahid Madani University is gratefully acknowledged. In addition the authors would like to thank the Drug Design Laboratory of Pharmacy Faculty of Tabriz University of medical sciences for providing the software and hardware needed for molecular docking and QSAR analysis.

## Abbreviations

| | |
|---|---|
| ZnO | zinc oxide |
| MgO | magnesium oxide |
| QSAR | quantitative structure activity relationship |
| LOOCV | leave one out cross-validation |
| MLR | multiple linear regression |
| [bmim]Cl | 1-buthyl-3-methyl imidazolium chloride |
| NMR | nuclear magnetic resonance |
| FT-IR | fourier transform infrared |
| LGA | Lamarckian genic algorithm |
| pNPG | 4-nitrophenyl-α-D-glucopyranoside |

## Appendix A. Supplementary data

Supplementary data related to this article can be found at http://dx.doi.org/10.1016/j.molstruc.2016.02.005.

## References


[1] T. Gungor, A. Fouquet, J.M. Teulon, D. Provost, M. Cazes, A. Cloarec, J. Med. Chem. 35 (1992) 4455–4463.
[2] E. Seyhan, N. Nilgun, A. Noyanalpan, N. Arzneim. Forsch. 47 (1997) 410.
[3] K.G. Desai, K.R. Desai, Bio. Med. Chem. 14 (2006) 8271–8279.
[4] Ö.Ö. Güven, T. Erdoğan, H. Göker, S. Yıldız, Bio. Med. Chem. 17 (2007) 2233–2236.
[5] R. Igual-Adell, C. Oltra-Alcaraz, E. Soler-Company, P. Sánchez-Sánchez, J. Matogo-Oyana, D. Rodríguez-Calabuig, Expert Opin. Pharmacother. 5 (2004) 2615–2619.
[6] W.A. Denny, G.W. Rewcastle, B.C. Baguley, J. Med. Chem. 33 (1990) 814–819.
[7] A.T. Mavrova, K.K. Anichina, D.I. Vuchev, J.A. Tsenov, P.S. Denkova, M.S. Kondeva, M.K. Micheva, Eur. J. Med. Chem. 41 (2006) 1412–1420.
[8] X. Diao, Y. Wang, Y. Jiang, D. Ma, J. Org. Chem. 74 (2009) 7974–7977.
[9] P.G. Baraldi, A. Bovero, F. Fruttarolo, D. Preti, M.A. Tabrizi, M.G. Pavani, R. Romagnoli, Med. Res. Rev. 24 (2004) 475–528.
[10] P. Chaudhuri, B. Ganguly, S. Bhattacharya, J. Org. Chem. 72 (2007) 1912–1923.
[11] R. Schiffmann, A. Neugebauer, C.D. Klein, J. Med. Chem. 49 (2006) 511–522.
[12] R.P. Verma, Bio. Med. Chem. 13 (2005) 1059–1067.
[13] M.L. Barreca, A. Chimirri, E. De Clercq, L. De Luca, A.M. Monforte, P. Monforte, A. Rao, M. Zappalà, 58 (2003) 259–263.
[14] S. Pal, W.-S. Hwang, I.J. Lin, C.-S. Lee, J. Mol. Catal. A Chem. 269 (2007) 197–203.
[15] P. Hao, S. Zhang, W.-H. Sun, Q. Shi, S. Adewuyi, X. Lu, P. Li, Organometallics 26 (2007) 2439–2446.
[16] J.A. Asensio, P. Gómez-Romero, Fuel Cells 5 (2005) 336–343.
[17] G. Schwartz, K. Fehse, M. Pfeiffer, K. Walzer, K. Leo, Appl. Phys. Lett. 89 (2006) 083503–083509.
[18] N. Singh, D.O. Jang, Org. Lett. 9 (2007) 1991–1994.
[19] D. Rajadhyaksha, D. Rangnekar, J. Chem. Technol. Biotechnol. 36 (1986) 300–304.
[20] A. Sannigrahi, D. Arunbabu, R.M. Sankar, T. Jana, 40 (2007) 2844–2851.
[21] Y. Ooyama, K. Yoshida, New J. Chem. 29 (2005) 1204–1212.
[22] I. Mohammadpoor-Baltork, A.R. Khosropour, S.F. Hojati, Cata. Commun. 8 (2007) 1865–1870.
[23] Y. Kim, M.R. Kumar, N. Park, Y. Heo, S. Lee, J. Org. Chem. 76 (2011) 9577–9583.
[24] K. Bahrami, M.M. Khodaei, I. Kavianinia, J. Chem. Res. 2006 (2006) 783–784.
[25] L.H. Du, Y.G. Wang, Synthesis (2007) 675–678.
[26] N.D. Kokare, J.N. Sangshetti, D.B. Shinde, 2007 (2007) 2829–2834.
[27] M. Chakrabarty, R. Mukherjee, S. Karmakar, Y. Harigaya, Monatsh. Chem. 138 (2007) 1279–1282.
[28] A.B. Alloum, K. Bougrin, M. Soufiaoui, Tetrahedron Lett. 44 (2003) 5935–5937.
[29] R. Varala, A. Nasreen, R. Enugala, S.R. Adapa, Tetrahedron Lett. 48 (2007) 69–72.
[30] Z.-H. Zhang, T.-S. Li, J.-J. Li, Monatsh. Chem. 138 (2007) 89–94.
[31] M.M. Heravi, M. Tajbakhsh, A.N. Ahmadi, B. Mohajerani, Monatsh. Chem. 137 (2006) 175–179.
[32] J.Y. Xu, H.P. Zhang, C.X. Yan, C.H. Zhou, W.H. Ma, L. Ma, Y. Yang, Adv. Mater. Res. Trans. Tech. Publ. 1092 (2015) 984–987.
[33] K. Sivakumar, V. Senthil Kumar, J.J. Shim, Y. Haldorai, Synth. React. Inorg. Met. Org. Nano-Met. Chem. 45 (2015) 660–666.
[34] D. Tumelty, M.K. Schwarz, K. Cao, M.C. Needels, Tetrahedron Lett. 40 (1999) 6185–6188.
[35] L. Dinparast, H. Valizadeh, E. Vessally, M.B. Bahadori, J. Mol. Struct. 1105 (2016) 118–127.
[36] L. Guczi, D. Horváth, Z. Pászti, L. Tóth, Z. Horváth, A. Karacs, G. Peto, J. Phys. Chem. B 104 (2000) 3183–3193.
[37] J.M. Thomas, Angew. Chem. Int. Ed. Engl. 33 (1994) 913–937.
[38] G. Santor, R. maryi, P. Righi, Chem. Ber. 104 (2004) 199.
[39] J.P. Hallett, T. Welton, Chem. Rev. 111 (2011) 3508–3576.
[40] H. Valizadeh, A. Azimi, J. Iran. Chem. Soc. 8 (2011) 123–130.
[41] Y. Chinthala, S. Thakur, S. Tirunagari, S. Chinde, A.K. Domatti, N.K. Arigari, K. Srinivas, S. Alam, K.K. Jonnala, F. Khan, Eur. J. Med. Chem. 93 (2015) 564–573.
[42] Y.G. Chen, P. Li, P. Li, R. Yan, X.Q. Zhang, Y. Wang, X.T. Zhang, W.C. Ye, Q.W. Zhang, Molecules 18 (2013) 4221–4232.
[43] M.J. Charron, R.A. Dubin, C.A. Michels, Mol. Cell. Biol. 6 (1986) 3891–3899.
[44] N. Asano, Glycobiology 13 (2003) 93R–104R.
[45] M. Yar, M. Bajda, S. Shahzad, N. Ullah, M.A. Gilani, M. Ashraf, A. Rauf, A. Shaukat, Bio. Chem. 58 (2015) 65–71.
[46] S. Atsumi, C. Nosaka, Y. Ochi, H. Iinuma, K. Umezawa, Cancer Res. 53 (1993) 4896–4899.
[47] D.P. Gamblin, E.M. Scanlan, B.G. Davis, Chem. Rev. 109 (2008) 131–163.
[48] A.J. Rawlings, H. Lomas, A.W. Pilling, M.J.R. Lee, D.S. Alonzi, J. Rountree, S.F. Jenkinson, G.W. Fleet, R.A. Dwek, J.H. Jones, ChemBioChem 10 (2009) 1101–1105.
[49] A. Mobinikhaledi, B. Asghari, M. Jabbarpour, Iran. J. Pharm. Res. 14 (2015) 723–731.
[50] E. Menteşe, S. Ülker, B. Kahveci, Chem. Heterocycl. Compd. (2014) 1820–1831.
[51] J.A. Kumar, A.K. Tiwari, A.Z. Ali, K. Madhusudhana, B.S. Reddy, S. Ramakrishna, B. China Raju, J. Enzyme Inhib. Med. Chem. 25 (2010) 80–86.
[52] L. Dinparast, H. Valizadeh, Monatsh. Chem. 146 (2015) 313–319.
[53] H. Valizadeh, L. Dinparast, Synth. Commun. 4 (2011) 291–294.
[54] H. Valizadeh, H. Gholipour, M. Mahmoudian, J. Iran. Chem. Soc. 8 (2011) 862–871.
[55] O.Z. Didenko, G.R. Kosmambetova, P.E. Strizhak, Chin. J. Catal. 29 (2008) 1079–1083.
[56] P.P. Roy, K. Roy, QSAR Comb. Sci. 27 (2008) 302–313.
[57] M.B. Bahadori, H. Valizadeh, B. Asghari, L. Dinparast, M.M. Farimani, S. Bahadori, J. Funct. Foods 18 (2015) 727–736.
[58] M. Frisch, G. Trucks, H. Schlegel, G. Scuseria, M. Robb, J. Cheeseman, J. Montgomery, T. Vreven Jr., K. Kudin, J. Burant, Gaussian 03, Revision C. 02 (Or D. 01), Gaussian, Inc., Pittsburgh PA, 2003.
[59] G.M. Morris, D.S. Goodsell, R.S. Halliday, R. Huey, W.E. Hart, R.K. Belew, A.J. Olson, J. Comput. Chem. 19 (1998) 1639–1662.
[60] M.F. Sanner, Python: a programming language for software integration and development, J. Mol. Graph. Model 17 (1999) 57–61.
[61] M. Taha, N.H. Ismail, S. Lalani, M.Q. Fatmi, S. Siddiqui, K.M. Khan, S. Imran, M.I. Choudhary, Eur. J. Med. Chem. 92 (2015) 387–400.
[62] S. Tatrdar, A. Jouyban, S. Soltani, M. Zakariazadeh, Pharm. Sci. 21 (2015) 86–93.
[63] R. Jahangiri, S. Soltani, A. Barzegar, Pharm. Sci. 20 (2014) 122–129.
[64] S. Soltani, H. Abolhasani, A. Zarghi, A. Jouyban, Eur. J. Med. Chem. 45 (2010) 2753–2760.